ELSEVIER

Thermochimica Acta 364 (2000) 111–119

thermochimica acta

www.elsevier.com/locate/tca

Physical chemistry of binary organic eutectic and monotectic alloys; durene–pyrogallol system

U.S. Rai*, Pinky Pandey

Chemistry Department, Faculty of Science, Banaras Hindu University, Varanasi-221 005, Uttar Pradesh, India

Received 15 May 2000; accepted 6 July 2000

Abstract

The phase-diagram of durene–pyrogallol system, determined by the thaw-melt method, shows the formation of a eutectic at 79.6°C and a monotectic at 127.7°C containing 0.95 and 0.05 mol fractions of durene, respectively. Growth data for the pure components, the eutectic and the monotectic, determined by measuring the rate of movement of solid–liquid interface in a capillary at different undercoolings (ΔT) suggest the applicability of Hillig–Turnbull equation, $v = u(\Delta T)^n$, where u and n are constants depending on the nature of materials involved. The values of enthalpy of fusion of the pure components, the eutectic and the monotectic were determined and from these values, the enthalpy of mixing, size of the critical nucleus, interfacial energy and excess thermodynamic functions were calculated. While optical microphotographs of the pure components showed a faceted microstructure, those of eutectic and monotectic show their characteristic features.

Keywords: Durene–pyrogallol system; Optical microphotographs; Enthalpy

1. Introduction

It is well known that investigations in the field of physics, chemistry, metallurgy and materials science dealing with the formation of eutectics, monotectics and addition compounds have been carried out for a long time, and in the process a variety of products of commercial and technological importance have been produced. The fundamental understanding of solidification process [1–8], and properties of polyphase alloys have been a subject of extensive theoretical and experimental investigations in the past decades. By this time it has become an established field of research as the current civilisation is in potential demand of newer materials with specific properties for particular applications but at the low cost. Although metallic eutectics, monotectics and intermetallic compounds constitute an interesting area of investigation [1–5], these systems pose a variety of problems in their investigations because of high transformation temperature involved, opacity of the metallic materials and difficulties involved in their purification. Besides, wide difference in densities of the two components forming the metal eutectics, monotectics and intermetallic compounds causes density driven convection effects, which in turn, affect their solidification. In view of these it was considered worth searching some transparent organic systems [9–14] to yield eutectic and monotectic. Hence, attention was focused on some organic systems in which the components could be easily purified, and their solidification behaviour involved low transition temperature, minimised

* Corresponding author. Tel.: +91-542-317190; fax: +91-542-217074.
E-mail address: usrai@banaras.emet.in (U.S. Rai).

0040-6031/00/$ – see front matter
PII: S0040-6031(00)00597-9

convection effect and possibility of visual examination of the solidification process due to transparency of the systems. As a consequence, the last couple of decades have seen a great zeal and interest and feverish activity in exploring some organic systems with regard to their physicochemical investigations which may ultimately help in producing novel materials in order to meet the current requirements.

A critical scanning of the existing literature [1–15] reveals that much less attention has been focused on the monotectic alloys because of limited choice of materials and considerable experimental difficulties associated with a liquid miscibility gap. In the present investigation both durene (D) and pyrogallol (PG) with enthalpy of fusion values 19.4 and 23.9 kJ mol^{-1}, respectively, are high heat of fusion compounds and a system involving these compounds will be an organic analog of a non-metal–non-metal system. With a view to elucidate the physical chemistry of this system, phase diagram, growth behaviour, thermochemistry and microstructure were studied.

2. Experimental

2.1. Materials and purification

While durene with more than 99% purity, was used as received in the present investigation, pyrogallol (S.D. Fine Chem. Pvt. Ltd., India) was purified by repeated distillation under reduced pressure. Purity of each compound was assessed by comparing its melting point with the values reported in the literature [16].

2.2. Phase-diagram

The phase-diagram of D–PG system was determined by the thaw-melt method [9,17]. In this method, mixtures of the two components covering the entire range of composition were prepared in long-necked test-tubes and these mixtures were homogenised by repeated melting followed by chilling in ice. The thawing and melting temperatures of these mixtures were determined by using Toshniwal melting point apparatus attached with a precision thermometer. A plot of composition on x axis and temperature on y axis gives the phase-diagram of the system under investigation.

2.3. Growth kinetics

The growth kinetics of D–PG system was studied [17–18] at different undercoolings by measuring the rate of movement of the solid–liquid interface in a capillary tube of U-shape with about 150 mm horizontal portion and 5 mm i.d. Molten pure components, eutectic and monotectic were separately placed in a capillary in a thermostat containing silicone oil. At any desired temperature below the melting point of the sample, a seed crystal of the same composition was added to start nucleation, and the rate of movement of the solid–liquid interface was measured using a travelling microscope and a stop watch.

2.4. Enthalpy of fusion

The values of enthalpy of fusion of pure components, the eutectic, and the monotectic were determined [19] by the Mettler DSC-4000 system. The instrument was calibrated using indium as a standard substance. The rate of heating and amount of sample were 10°C and 5 mg, respectively, for each estimation. The percentage error in the enthalpy of fusion values was $\pm 1.0\%$.

2.5. Microstructure

Optical microphotographs of the pure components, the eutectic, and the monotectic were recorded [20] by placing small amount of the molten compound on a well washed and dried glass slide. The coverslip was slipped over the molten liquid and when temperature of the sample was below its melting temperature, a seed crystal of the same compound was added to facilitate the solidification process. Care was taken to see that the solidification was unidirectional. When solidification was complete, the slide was placed on the platform of a Leitz Laborlux D optical microscope, different regions were viewed and interesting regions were photographed with the camera attached to the microscope.

3. Results and discussion

3.1. Phase-diagram

The phase-diagram of D–PG system is given in Fig. 1 in the form of composition versus melting

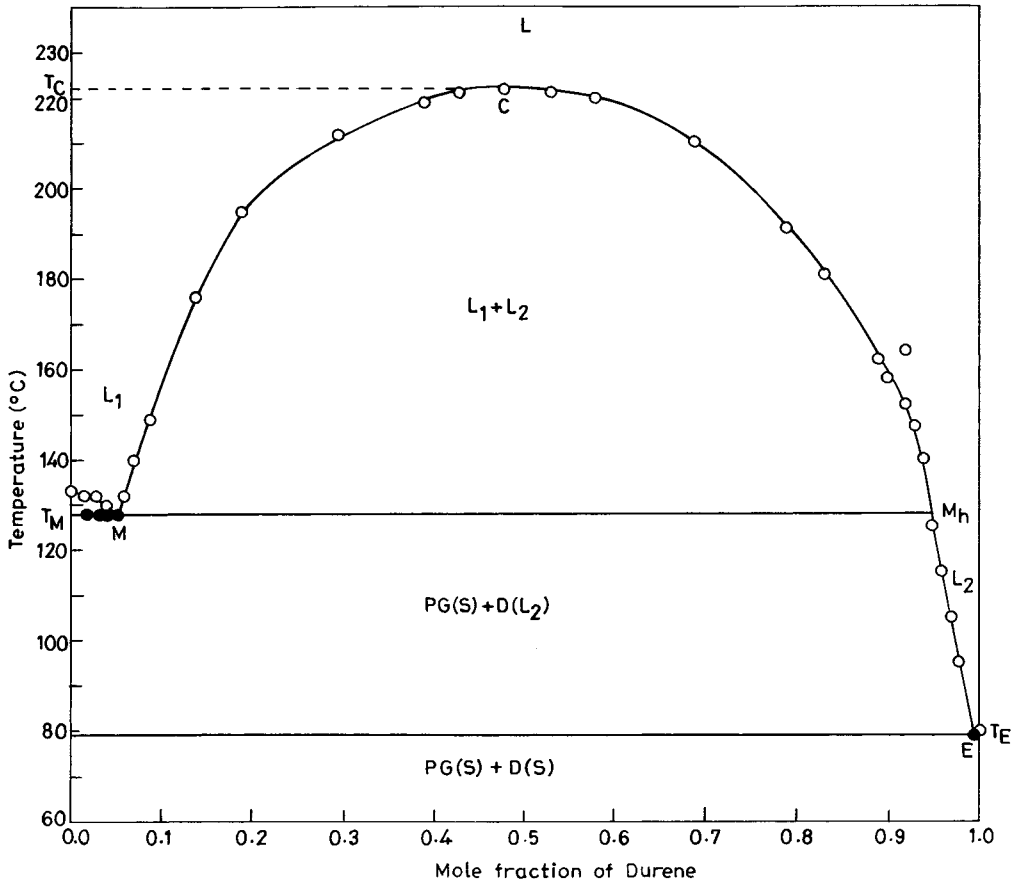

Fig. 1. Phase-diagram of durene–pyrogallol system: (○) melting temperature; (●) thaw temperature.

temperature plots. The melting point of pyrogallol is 133.0°C and addition of durene to it reduces the melting temperature to a limited extent in a short range of composition until the monotectic temperature T_M is attained. Beyond this composition, a slight addition of the second component produces immiscibility. The region [21–22] $L_1 + L_2$ bounded by MCM_h shows the wide range of composition where the two components are completely immiscible. The immiscibility temperature goes on increasing with composition until a maximum temperature T_C is attained above which the two liquids are miscible in all proportions. This temperature is known as the critical solution temperature (T_C). After attaining the critical solution temperature, the miscibility temperature again decreases with addition of durene until the eutectic temperature T_E is attained. The $L_1 + L_2$ region is regarded as being made up of an infinite number of tie lines which connect the two liquid phases L_1 and L_2. With increasing temperature, the tie lines become progressively smaller until the ultimate tie-line at the top of MCM_h curve has more or less zero length, and corresponds with the critical solution temperature or consolute temperature (T_C).

When a liquid of monotectic composition is cooled below the monotectic horizontal, the monotectic reaction [23] occurs and a liquid L_1 which is rich in pyrogallol decomposes into a solid phase being rich in the first component (pyrogallol) and another liquid phase L_2 rich in the second component durene. The process at the monotectic temperature can be represented as

$$L_1 \rightleftharpoons S_1 + L_2$$

When a liquid of eutectic composition is allowed to cool below the eutectic temperature (T_E), the eutectic crystallisation produces two solids (S_1 rich in pyrogallol and S_2 rich in durene) and is represented by the following equation:

$$L_2 \rightleftharpoons S_1 + S_2$$

Thus, the monotectic process is similar to the eutectic except that one of the product phases of the monotectic is a second liquid phase. The eutectic, the monotectic and the consolute temperatures are 79.6, 127.7 and 222.0°C, respectively.

3.2. Growth kinetics

With a view to study, the growth kinetics of D–PG system, linear velocities of crystallisation (v) of the pure components, the eutectic and the monotectic were determined at different undercooling temperatures (ΔT) by measuring the rate of movement of solid–liquid interface in a capillary. The crystallisation rates are given in Table 1 and the plots of log v against log ΔT are shown in Fig. 2. The linear dependence of these plots is in accordance with the Hillig and Turnbull [24] equation

$$v = u(\Delta T)^n \quad (1)$$

where u and n are the constants depending on the solidification behaviour of the materials under investigation. The experimental values of these constants are given in Table 1. The basic criterion [25] for the determination of growth mechanism is the comparison of the temperature dependence of linear velocity of crystallisation with the theoretically predicted equations. While normal growth generally occurs on the rough interface in which case there is direct proportionally between crystallisation velocity and undercooling, lateral growth is facilitated by the presence of steps, jogs, bends, etc. and under such conditions, the relationship for the spiral mechanism follows the parabolic law given by Eq. (1). In the majority of cases n assuming a value more than one suggests that in such cases the growth mechanism obeys the parabolic law. In case of the monotectic the value of n being quite close to one suggests direct proportionally between growth velocity and undercooling. This expected deviation may be due to difference in diffusion of components to the solidification site and different mode of heat conduction through the liquid phase present in the case of the monotectic. It is evident from the data given in the Table 1 that the growth velocity of eutectic and monotectic is more than those of the pure components. Also, the growth velocity of the monotectic is higher than that of the eutectic. This difference may be ascribed to the difference in heat flow and the diffusion mode during monotectic and eutectic solidification.

Table 1
Values of u and n for pure components, eutectic and monotectic

Material	u (mm s^{-1} deg^{-1})	n
Durene (D)	2.8×10^{-2}	3.6
Pyrogallol (PG)	1.2×10^{-4}	4.7
D–PG eutectic	3.1×10^{-1}	2.3
D–PG monotectic	9.7×10^{-1}	0.8

3.3. Thermochemistry

The process of solidification is comprised of two stages [26], namely, nucleation and growth. While nucleation depends on solid–liquid interface energy which can be calculated from the heats of fusion, the growth step depends on the manner in which particles from liquid phase are added on to the solid–liquid interface, which is determined by the structure of the interface. The interface structure, in turn, depends on the entropy of fusion of the material under investigation and the thermal environment in which the crystal grows. Thus, the heats of fusion of pure components and eutectics are very important in understanding the mechanism of solidification. In addition, different thermodynamic quantities such as entropy of fusion, interfacial energy, enthalpy of mixing and excess thermodynamic functions can be calculated from the heat of fusion data.

The values of enthalpy of fusion determined by the DSC method are given in Table 2. If a eutectic is a simple mechanical mixture of two components not involving any type of association in the melt, the heat of fusion may simply be calculated by the mixture law [27]

$$(\Delta_f h)_e = x_1 \Delta_f h_1^o + x_2 \Delta_f h_2^o \quad (2)$$

where x and $\Delta_f h$ are the mole fraction and enthalpy of fusion of the component indicated by the subscript,

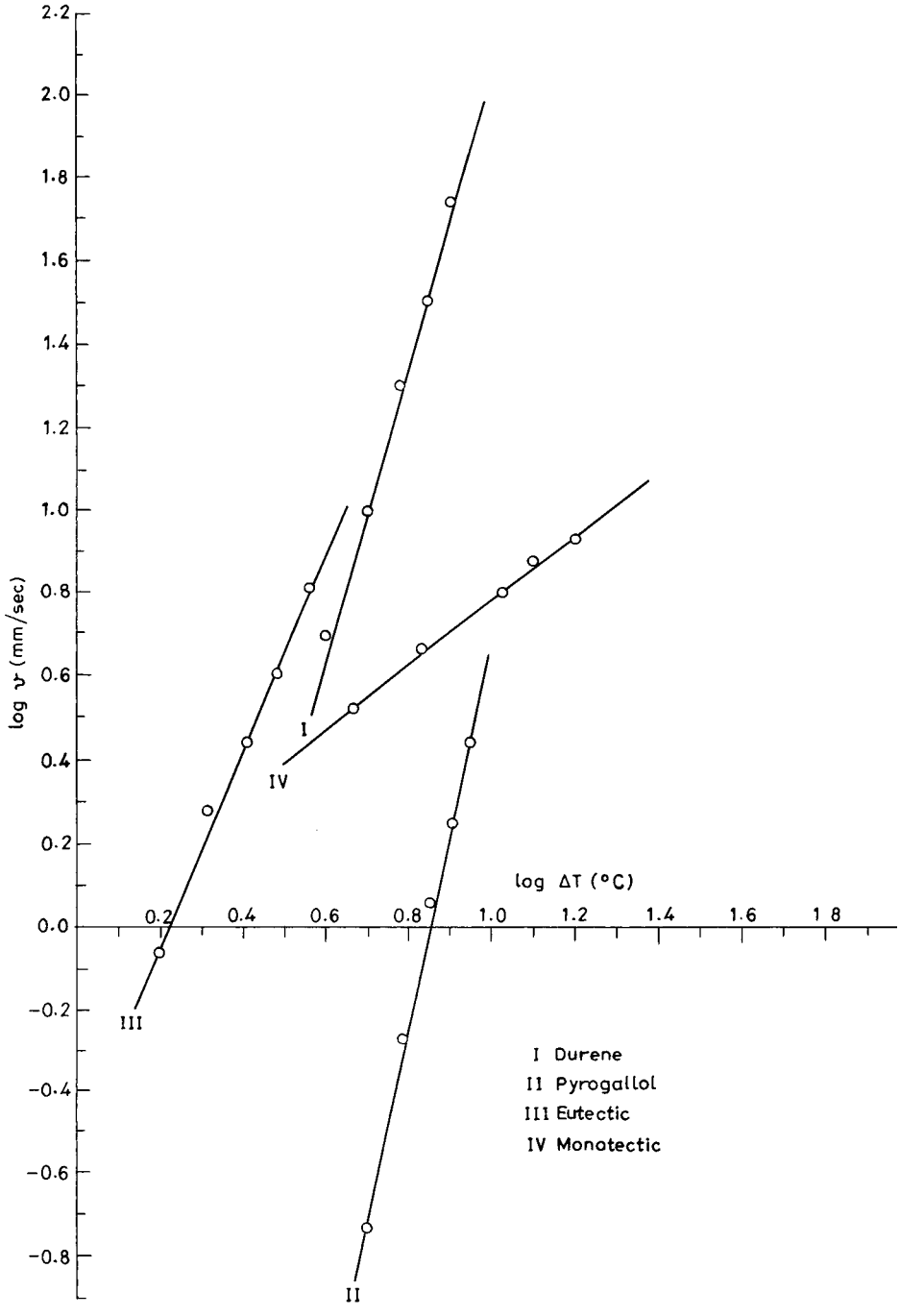

Fig. 2. Linear velocity of crystallization of durene, pyrogallol, their eutectic and monotectic.

Table 2
Heat of fusion, entropy of fusion and jackson's roughness parameter

Material	Heat of fusion (kJ mol^{-1})	Entropy of fusion (J mol^{-1} K^{-1})	Roughness parameter ($\alpha = \Delta_f S/R$)
Durene (D)	19.4	55.0	6.6
Pyrogallol (PG)	23.9	58.9	7.1
D–PG eutectic (experimental)	21.4	60.8	7.3
D–PG eutectic (calculated)	19.5		
D–PG monotectic (experimental)	19.7	49.2	5.9

respectively. For the purpose of comparison the calculated values of heat of fusion are also given in Table 2 along with their experimental data. The value of enthalpy of mixing, $\Delta_m H$, of the eutectic is given by the following equation [28]:

$$\Delta_m H = (\Delta_f h)_{\text{expt.}} - (\Delta_f h)_{\text{calc.}}$$

where $(\Delta_f h)_{\text{expt.}}$ is the heat of fusion determined experimentally and $(\Delta_f h)_{\text{calc.}}$ is its corresponding calculated value. It is evident that the enthalpy of mixing of the eutectic is $+1.9$ kJ mol^{-1}. Thermochemical studies [29] suggest that the structure of binary eutectic melt depends on the sign and magnitude of heat of mixing. As such, three types of structures are suggested: (i) quasieutectic for which $\Delta_m H > 0$, (ii) clustering of molecules, in which $\Delta_m H < 0$, and (iii) molecular solutions, for which $\Delta_m H = 0$. The value of enthalpy of mixing being $+1.9$ kJ mol^{-1} suggests that there is quasieutectic structure in the binary organic eutectic melt.

The deviation from ideal behaviour can best be expressed in terms of excess thermodynamic functions which give more quantitative idea about the nature of molecular interactions. It is given by the difference between the thermodynamic functions of mixing for a real system and the corresponding values for an ideal system at the same temperature and pressure. It is denoted by superscript E and represents the excess of a given thermodynamic property of a solution over that in the ideal solutions. In order to know the nature of interaction between the components forming the eutectic melt, some thermodynamic functions such as excess free energy (g^E), excess enthalpy (h^E) and excess entropy (s^E) were calculated using the following equations [30]:

$$g^E = RT(x_1 \ln \gamma_1^l + x_2 \ln \gamma_2^l) \tag{3}$$

$$h^E = -RT^2 \left(x_1 \frac{\partial \ln \gamma_1^l}{\partial T} + x_2 \frac{\partial \ln \gamma_2^l}{\partial T} \right) \tag{4}$$

$$s^E = -R \left(x_1 \ln \gamma_1^l + x_2 \ln \gamma_2^l + x_1 T \frac{\partial \ln \gamma_1^l}{\partial T} + x_2 T \frac{\partial \ln \gamma_2^l}{\partial T} \right) \tag{5}$$

The activity coefficient of a component i present in the eutectic melt is given by

$$-\ln x_i^l \gamma_i^l = \frac{\Delta_f h_i^o}{R} \left(\frac{1}{T} - \frac{1}{T_i^o} \right) \tag{6}$$

where $x_i^l, \gamma_i^l, \Delta_f h_i^o$, and T_i^o are respectively the mole fraction, activity coefficient, heat of fusion and the melting temperature of the component i, R is the gas constant and T is the melting temperature of the eutectic. Eq. (6) is obtained assuming the general condition of phase equilibrium for the phases and that heat of fusion is independent of temperature and the two components are miscible in all proportion in the liquid phase only. The values of $\partial \ln (\gamma_i^l / \partial T)$ can be calculated [31] by taking the slope of the liquidus curve near the eutectic point in the phase diagram and using Eq. (7) which is obtained by differentiating Eq. (6),

$$\frac{\partial \ln \gamma_i^l}{\partial T} = \frac{\Delta_f h_i^o}{RT^2} = \frac{1}{x_i} \frac{\partial x_i}{\partial T} \tag{7}$$

Since the liquidus curves in the phase diagram are virtually straight lines in the region of the eutectic composition, the values of $\partial x_i / \partial T$ has been found out by measuring their slope near the eutectic point. The values of excess functions are given in Table 3. The excess free energy, g^E, being positive suggests [32] that there is weak interaction among the components forming the eutectic melt and strong association between like molecules. Thus, D–D or PG–PG

Table 3
Excess thermodynamic functions for the eutectic

Material	g^E (J mol^{-1})	h^E (kJ mol^{-1})	s^E (J mol^{-1} K^{-1})
D–PG eutectic	100.1	−8.5	24.4

association is stronger than that of D–PG attractive interactions. The values of h^E and s^E, very much related to g^E are, respectively, a measure of excess enthalpy and excess entropy of mixing.

The values of entropy of fusion ($\Delta_f S$), calculated with the help of Eq. (8) are reported in Table 3, further lend support to the inference drawn from the excess thermodynamic data with regards to structure, stability and ordering in the melts. The values of entropy of fusion ($\Delta_f S$) of the pure components, the eutectic and the monotectic were calculated using the following equation [30]:

$$\Delta_f S = \frac{\Delta_f h}{T} \tag{8}$$

where $\Delta_f h$ is the heat of fusion and T is the fusion temperature on absolute scale. In all the cases under investigation, $\Delta_f S$ values are positive, indicating an increase in randomness during melting of different phases.

The interfacial tension affects the magnitude of heat of fusion. The solid–liquid interface plays an important role in determining the kinetics of phase transformation. During the growth of a crystal, the radius of critical nucleus is influenced by undercooling as well as the interfacial energy of the surface involved. The interfacial energy (σ) is given by the equation [26]

$$\sigma = \frac{C\,\Delta_f h}{(N)^{1/3}(V_m)^{2/3}} \tag{9}$$

where N is the Avogadro number, V_m is the molar volume and C is a constant assuming values between 0.30 and 0.35. The values of interfacial energy using Eq. (9) are given in Table 4.

The past decade has witnessed several articles [26,28,33] with various attempts to understand and explain the process of solidification of monotectic alloys. The role of wetting, in particular, in phase separation process is of potential importance in the present context. Due to this, the applicability of Cahn's wetting condition has been put to test in this system. The perfect wetting of the solid phase is supported by the condition,

$$\sigma_{SL_2} < \sigma_{SL_1} + \sigma_{L_1L_2} \tag{10}$$

where σ is the interfacial energy between the faces denoted by the subscript. The value of $\sigma_{L_1L_2}$ has been calculated using the equation [34]

$$\sigma_{L_1L_2} = \sigma_{SL_1} + \sigma_{SL_2} - 2\sqrt{\sigma_{SL_1}\sigma_{SL_2}} \tag{11}$$

The data given in Table 4 justify the validity of Cahn's wetting condition for the monotectic system under investigation.

Table 4
Interfacial energy values for durene, pyrogallol and their monotectic

Parameters	Value (ergs cm^{-2})
SL_1 (D)	30.7
SL_2 (PG)	64.1
L_1L_2 (D–PG)	6.1

When a melt is cooled below its equilibrium melting temperature, the liquid phase does not solidify directly but in stages, named nucleation and growth. It is well known that under equilibrium condition the melt contains large number of clusters of molecules. So long as the clusters are all below the critical size, they can not grow to form crystals and the critical size radius (r^*) of nucleus may be calculated [26] by

$$r^* = \frac{2\sigma T_m}{\Delta_f h\,\Delta T} \tag{12}$$

where T_m, $\Delta_f h$ and ΔT are melting temperature, heat of fusion per mol and degree of undercooling, respectively. The values of size of critical nucleus calculated on the basis of Eqs. (9) and (12) are reported in Table 5. It is evident from the reported data that the critical radius (r^*) is inversely proportional to under cooling ΔT. This may be ascribed [35] to the increased amplitude of atomic vibration at the higher temperatures.

3.4. Microstructure

It is well known that the microstructure [35] of a polyphase material gives size, shape and distribution of phases. It is of immense importance in deciding mechanical, electrical, magnetic, and optical properties of materials. In general, properties of materials are functions of their microstructures. Desired type of

Table 5
Radius of critical nucleus at different degrees of undercoolings

Undercooling (ΔT) (°C)	D	PG	Eutectic	Monotectic
1.6			6.4	
2.1			4.9	
2.6			3.9	
3.1			3.3	
3.6			2.8	
4.3	2.6			
4.7				5.4
5.0		4.4		
5.3	2.1			
6.0		3.6		
6.3	1.8			
6.7				3.8
7.0		3.1		
7.3	1.5			
8.0		2.7		
8.3	1.3			
9.0		2.4		
10.7				2.4
12.7				2.0
15.7				1.6

microstructures, generating required properties, can be obtained by controlling the solidification process, addition of small amount of impurities and selecting appropriate combination of materials, besides other variables, e.g. entropy of fusion, the solid–liquid phase structure and the undercooling which have a pronounced effect on the microstructure of alloys.

The microstructural features of the eutectic given in Figs. 3 and 4 indicate a lamellar eutectic morphology. The overall growth features indicate the formation of eutectic dendrites. The secondary arms appear to align at an angle of about 45° from the main stem of the dendrites. In the microstructure of the monotectic (Fig. 5) the seed phase also grows like one of the constituents of the eutectic phase. The two phases appear to have grown perpendicular to each other.

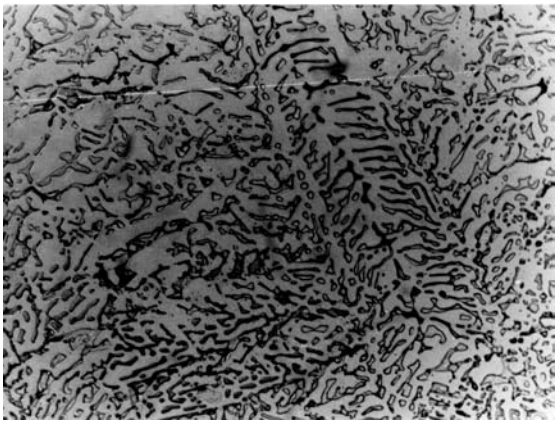

Fig. 3. Microstructure of eutectic × 500.

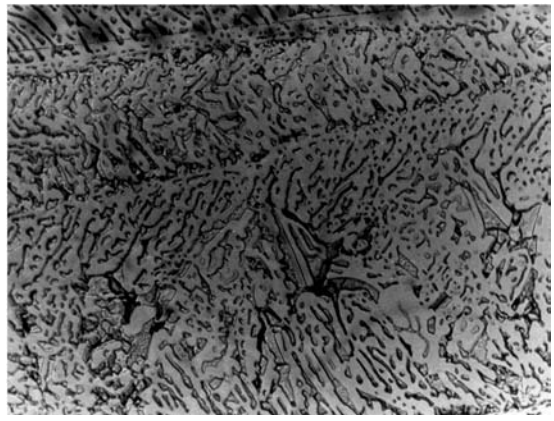

Fig. 4. Microstructure of eutectic × 500.

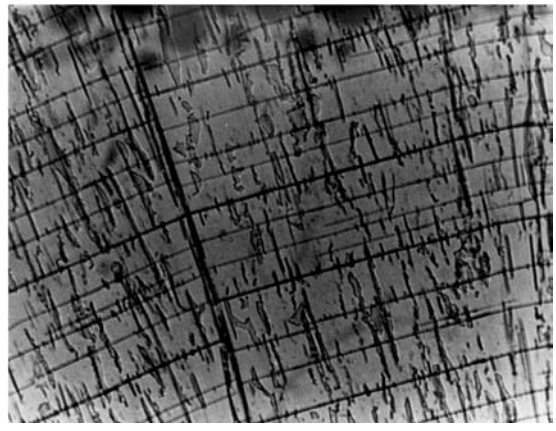

Fig. 5. Microstructure of monotectic × 500.

Acknowledgements

Thanks are due to UGC, New Delhi for financial assistance.

References

[1] J. Liu, R. Elliott, J. Cryst. Growth 162 (1996) 107.
[2] D.M. Herlach, R.F. Cochrane, I. Egry, H.J. Fecht, A.L. Greer, Int. Mater. Rev. 38 (1993) 273.
[3] J. Glazer, Int. Mater. Rev. 40 (1995) 65.
[4] M.R. Aguiar, R. Cram, J. Cryst. Growth 162 (1996) 107.
[5] R. Elliott, Eutectic Solidification Processing, Butterworths, London, 1983.
[6] W. Kurz, R. Trivedi, in: Proceedings of the Third International Conference on solidification Processing, Sheffield, 1987, p. 1.
[7] R.S. Sokolowski, M.E. Glicksman, J. Cryst. Growth 119 (1992) 126.
[8] J. Seth, W.R. Wilcox, J. Cryst. Growth 114 (1991) 357.
[9] J. Sangster, J. Phys. Chem. Ret. Data 23 (1994) 295.
[10] H. Yasuda, I. Ohnaka, Y. Matsunaga, Y. Shiohara, J. Cryst. Growth 158 (1996) 128.
[11] R.P. Rastogi, N.B. Singh, K.D. Dwivedi, Ber. Bun-Senges Phys. Chem. 85 (1981) 85.
[12] H. Song, A. Hellawell, Metall. Trans. 20A (1989) 171.
[13] B.M. Shukla, N.P. Singh, N.B. Singh, Mol. Cryst. Liq. Cryst. 104 (1984) 265.
[14] J.E. Smith, D.O. Frazier, W.F. Kaukler, Scripta Metall. 18 (1984) 677.
[15] U.S. Rai, K.D. Mandal, Can. J. Chem. 62 (1989) 239.
[16] J.A. Dean, Lange's Handbook of Chemistry, McGraw-Hill, New York, 1985.
[17] U.S. Rai, K.D. Mandal, Bull. Chem. Soc. Jpn. 63 (1990) 1496.
[18] U.S. Rai, R.N. Rai, Chem. Mater. Am. Chem. Soc., in press.
[19] J.W. Dodd, K.H. Tonge, in: B.R. Currell (Ed.), Thermal Methods, Analytical Chemistry by Open Learning, Wiley, New York, 1987, p. 120.
[20] U.S. Rai, H. Shekhar, Thermochim. Acta 175 (1991) 215.
[21] F.N. Rhines, Phase Diagrams in Metallurgy, McGraw Hill, Inc., New York, 1956, p. 72.
[22] J.B. Andrews, A.C. Sandlin, P.A. Curreri, Metall. Trans. 19A (1988) 2651.
[23] U.S. Rai, R.N. Rai, J. Cryst. Growth 191 (1998) 234.
[24] W.B. Hillig, D. Turnbull, J. Chem. Phys. 24 (1956) 91.
[25] D.A. Porter, K.E. Easterling, Phase Transformations in Metals and Alloys, Van Nostrand Reinhold, New York, 1982.
[26] U.S. Rai, R.N. Rai, J. Mater. Res. 14 (1999) 1299.
[27] U.S. Rai, S. George, Thermochim. Acta 243 (1994) 17.
[28] U.S. Rai, P. Pandey, Mater. Lett. 39 (1999) 166.
[29] N. Singh, N.B. Singh, U.S. Rai, O.P. Singh, Thermochim. Acta 95 (1985) 291.
[30] U.S. Rai, R.N. Rai, Mol. Mater. 9 (1998) 235.
[31] U.S. Rai, O.P. Singh, N.P. Singh, N.B. Singh, Thermochim. Acta 71 (1983) 373.
[32] J. Wisniak, A. Tamir, Mixing and Excess Thermodynamic Functions (A Literature Source Book), Physical Science Data, Elsevier, New York, 1978.
[33] N.B. Singh, U.S. Rai, O.P. Singh, J. Cryst. Growth 71 (1985) 353.
[34] R. Good, Ind. Eng. Chem. 62 (1970) 54.
[35] G.A. Chadwick, Metallography of Phase Transformation, Butterworths, London, 1972.